

REPORT DOCUMENTATION PAGE

1a. REPORT SECURITY CLASSIFICATION Unclassified		1b. RESTRICTIVE MARKINGS None	
2a. SECURITY CLASSIFICATION AUTHORITY N/A		3. DISTRIBUTION/AVAILABILITY OF REPORT Unlimited.	
2b. DECLASSIFICATION/DOWNGRADING SCHEDULE N/A		5. MONITORING ORGANIZATION REPORT NUMBER(S)	
AD-A243 257 ORGANIZATION Cornell University		6b. OFFICE SYMBOL (If applicable) N/A	
7a. NAME OF MONITORING ORGANIZATION Office of Naval Research		7b. ADDRESS (City, State, and ZIP Code) Resident Representative N62927 Administrative Contracting Officer 33 Third Avenue - Lower Level New York, NY 10003-0000	
8a. NAME OF FUNDING/SPONSORING ORGANIZATION Department of the Navy		8b. OFFICE SYMBOL (If applicable)	
9. PROCUREMENT INSTRUMENT IDENTIFICATION NUMBER N00014-89-J-1311		10. SOURCE OF FUNDING NUMBERS	
8c. ADDRESS (City, State, and ZIP Code) Office of the Chief of Naval Research 800 North Quincy Street, Code 1513:CMB Arlington, VA 22217-5000		PROGRAM ELEMENT NO.	PROJECT NO.
		TASK NO.	WORK UNIT ACCESSION NO.
11. TITLE (Include Security Classification) "Innovative Optoelectronic Materials and Structures using OMVPE"			
12. PERSONAL AUTHOR(S) James R. Shealy			
13a. TYPE OF REPORT Annual Report	13b. TIME COVERED FROM 1/1/91 TO 11/25/91	14. DATE OF REPORT (Year, Month, Day) 91/11/25	15. PAGE COUNT
16. SUPPLEMENTARY NOTATION			
17. COSATI CODES		18. SUBJECT TERMS (Continue on reverse if necessary and identify by block number)	
FIELD	GROUP	SUB-GROUP	
		Semiconductors, Optoelectronics, Crystal Growth	
19. ABSTRACT (Continue on reverse if necessary and identify by block number) An advanced OMVPE process is being developed for the deposition of III-V semiconductor materials and structures. There are important optoelectronic device structures which can not be realized by conventional means. These include AlGaAs semiconductor lasers with improved coherence using embedded diffraction gratings, and GaInP pseudomorphic structures on GaP substrates for short wavelength semiconductor lasers. The structure on GaP result in improved laser performance compared to the 650 nm AlGaInP devices previously developed in this program. The new OMVPE apparatus combines the multichamber reaction cell with deep UV photo-assisted growth and modulation flow epitaxial techniques. Using a combination of such processes, the growth temperature requirements for III-V alloys can be substantially reduced. Selective growth on a sub-micron scale will be attempted with in-situ interference holography. The materials and techniques developed in this research program will result in significant simplifications to the fabrication sequence required to realize complex integrated optoelectronic circuits.			
20. DISTRIBUTION/AVAILABILITY OF ABSTRACT <input checked="" type="checkbox"/> UNCLASSIFIED/UNLIMITED <input type="checkbox"/> SAME AS RPT. <input type="checkbox"/> DTIC USERS		21. ABSTRACT SECURITY CLASSIFICATION N/A	
22a. NAME OF RESPONSIBLE INDIVIDUAL James R. Shealy		22b. TELEPHONE (Include Area Code) 22c. OFFICE SYMBOL (607) 255-4657	

1991 Progress Report

This report documents the progress during the period from Jan. 1 to November 25, 1991 on the SDIO/IST Electronic Materials Program under the direction of Professor J.R. Shealy at Cornell University. Currently the program has been funded through September 31, 1991. This report briefly describes the progress during this period in 3 principal areas, the construction of Cornell's OMVPE facility and the SDI OMVPE reactor, the use of selective heterostructure disordering techniques for OEIC applications, and the growth and characterization of (AlAs)(InAs) ordered epitaxial structures on InP by Migration Enhanced Epitaxy.

OMVPE Facility & SDIO Reactor Construction

Cornell's OMVPE facility has been completed and approved by the N.Y. State agency, the Department of Environmental Conservation (DEC), for operation with concentrated arsine and phosphine sources. Secondary hydride containment systems have been tested and are currently in use. The first OMVPE reactor to come on line (the machine donated by GE) has been leaked checked, baked with HCl gas, and completely interfaced to a computer for run automation. The first run will take place in early December 1991 shortly after the arsine bottle arrives. All other sources are in place including TEG, TMAA, and the carbon and tellurium dopants. The SDIO reactor construction has received the full time attention of 2 graduate students, one supported by a NSF fellowship. The deep UV coherent laser system is ready to be operated and optica are currently on order to perform preliminary studies in PMMA on Si to determine the ultimate pattern resolution for this excitation source using focused spot and interference holographic techniques. The re-designed reaction cell is currently being installed and leaked checked. Apart from the reaction cell, all that remains is a portion of the gas handling system and the electronics for manual and computer aided operation.

OEIC Fabrication Using Selective Heterostructure Disordering

The selective heterostructure disordering techniques developed earlier in this program were recently applied to the fabrication of a Surface Emitting Ring Laser OEIC in collaboration with David Sarnoff Research Laboratory. These devices have an gain region which is electrically pumped and a passive Bragg grating region used for coupling the radiation normal to the surface. The concept was to disorder the passive grating regions to increase their effective bandgap to reduce absorption losses. Currently these devices are under test to evaluate the effectiveness of this method for enhancing device performance.

Growth & Characterization of AlInAs by MEE

Raman scattering x-ray diffraction and transmission electron microscopy (TEM) have been used to study material composition, structure and strain in $(\text{InAs})_1(\text{AlAs})_2$ and $(\text{InAs})_2(\text{AlAs})_2$ superlattices grown on InP (001) substrates by Migration Enhanced Epitaxy (MEE). The energies of the observed zone folded acoustic and quantum confined optic phonons are in reasonable agreement with calculations based on one dimensional

91-17458**91 1209 135**

elastic continuum and linear chain models. The x-ray diffraction and TEM data confirm the existence of superperiodicity and support the Raman scattering results. This study represents the first report of ordered AlInAs alloys grown by any epitaxial method. The reduced growth temperature offered by MEE provides compatibility with the low growth temperatures needed for GaInAs alloys.

Interaction with the SDIO Program at JPL

In addition to these technical tasks it should be noted that efforts have been made to interact with the SDIO program at JPL. This has taken the form of a visit by Prof. Shealy (hosted by Satish Khanna) to JPL's fabrication facility to learn about their materials needs from Robert J. Lang. Also, Barbara Wilson has visited Cornell's OMVPE facility as part of JPL's recruitment activities. It has become clear that JPL's program requires epitaxial materials on InP for a demonstration of a WDM OEIC at 1.3 and 1.5 μm . As a result, materials in the AlGaInAs system will be prepared on InP using the presently running OMVPE reactor at Cornell. This effort represents a new materials thrust in this program, but this can be accommodated with existing funding until the SDIO reactor comes on line in the 2nd quarter of 1992.

Accession For	
NTIS GRA&I	<input checked="" type="checkbox"/>
DTIC TAB	<input type="checkbox"/>
Unannounced	<input type="checkbox"/>
Justification	
By	
Distribution/	
Availability Codes	
Avail and/or	
Dist	Special
A-1	

Characterization by Raman scattering, x-ray diffraction
and transmission electron microscopy
of $(\text{AlAs})_m(\text{InAs})_m$ short period superlattices grown by
migration enhanced epitaxy

J. Bradshaw[†], X. J. Song, J. R. Shealy
School of Electrical Engineering
Phillips Hall, Cornell University
Ithaca, NY 14853-5401

H. Østergaard
Technical University of Denmark

[†]current address: Photonics Research Laboratory, Dept. of Chemistry, SUNY at
Buffalo, Buffalo, NY 14217

Raman scattering, x-ray diffraction and transmission electron microscopy (TEM) have been used to study material composition, structure and strain in $(\text{InAs})_1(\text{AlAs})_1$ and $(\text{InAs})_2(\text{AlAs})_2$ superlattices grown on InP (001) substrates by migration-enhanced epitaxy (MEE). The energies of the observed zone folded acoustic and quantum confined optic phonons are in reasonable agreement with calculations based on one dimensional elastic continuum and linear chain models. The x-ray diffraction and TEM data confirm the existence of superperiodicity and support the Raman scattering results.

Short period superlattices (SPS) have found application as replacements for the corresponding alloy in several III-V materials systems because the ordered structure reduces charge scattering and exciton broadening, due, respectively, to alloy potential fluctuations and clustering caused by immiscibility.^{1,2} $\text{In}_{.53}\text{Ga}_{.47}\text{As}$ and $\text{In}_{.52}\text{Al}_{.48}\text{As}$ lattice matched to InP have shown promise in modulation doped field effect transistors and high speed optical modulators because of high electron mobility, large band-edge discontinuity and large $\Gamma - X$ valley separation.³⁻⁶ Although the lattice mismatch between the binary compounds in both systems complicates epitaxial growth, several groups have successfully grown high quality $(\text{InAs})_m(\text{GaAs})_n$ strained layer superlattices by molecular beam epitaxy (MBE) or organometallic vapor phase epitaxy (OMVPE).⁷⁻¹⁰

Alternate deposition of metal atoms and As_4 molecules at reduced temperatures (200–500 °C) results in layers with superior uniformity and interface abruptness.¹¹ Under these conditions, surface migration of both group III and group V species is increased, and three dimensional island growth is suppressed. Since MEE results in monolayer by monolayer growth, it is ideal for epitaxy of SPS structures. Recently it has been used to fabricate strained layer $(\text{InAs})_m(\text{GaAs})_n$ layers with improved structural and optical characteristics.¹⁰ In this letter, we describe the application of MEE to growth of high quality mono- and bilayer superlattices in the $(\text{InAs})(\text{AlAs})$ system. Because of the relatively high activation energy of Al (≈ 1.6 eV), in conventional MBE it is desirable

to grow Al containing compounds at elevated temperatures (680–720 °C) in order to allow surface migration. Growth of InAs, on the other hand, requires substrate temperatures lower than 500 °C to prevent In desorption. Since MEE allows enhanced surface migration of all group III species at low temperature, it would seem to be well suited for this system. To date, there has been at least one report of MBE growth of this structure,¹² but, to the best of the authors' knowledge, this is the first report of MEE growth of $(\text{InAs})_m(\text{AlAs})_m$.

$(\text{InAs})_1(\text{AlAs})_1$ and $(\text{InAs})_2(\text{AlAs})_2$ were grown on InP (001) substrates by MEE at 400 °C in a computer controlled Varian Gen II. Prior to growth, the native oxide was removed by thermal desorption at 500 °C. After deposition of a 2000 Å $\text{In}_{.52}\text{Al}_{.48}\text{As}$ buffer layer, 100 periods of $(\text{InAs})_1(\text{AlAs})_1$ or 50 periods of $(\text{InAs})_2(\text{AlAs})_2$ were grown, giving a total superlattice thickness of 600 Å in each case. This is below the critical thickness of 920 Å for $\text{In}_{.50}\text{Al}_{.50}\text{As}$, the average SPS composition, which is lattice mismatched to InP by 0.16%.¹³ Finally, a 500 Å $\text{In}_{.52}\text{Al}_{.48}\text{As}$ cap layer was grown. The group III beam fluxes were 3×10^{14} atoms/cm²sec, corresponding to a growth rate of 0.5 monolayer/sec. A clear streak RHEED pattern which alternated between 2×4 (As stabilized surface) and 4×2 (metal stabilized surface) persisted without attenuation, indicating that uniform two dimensional growth persisted throughout.¹⁴

Raman spectroscopy has developed into a powerful characterization technique for compound semiconductor materials and heterostructures. In particular, superlattices display quantum confined optical and zone folded acoustic

phonons which are highly sensitive to layer thickness and interface quality.^{15,16} Raman spectra were taken in backscattering geometry from the (001) crystal face using the 488 or 476 nm line of an Ar⁺ laser. The incident laser power density was on the order of 100 W/cm². A triple grating spectrograph, Si photodiode array and optical multichannel analyzer were used to record and analyze the data. The sample was placed in a liquid nitrogen cryostat at approximately 100 °K to narrow spectral linewidths and to avoid scattering by air. A polarization rotater and analyzer were used to select the desired polarization of the incident and scattered light. Before entering the spectrograph, the polarization of the scattered light was scrambled to avoid spurious results arising from the polarization sensitivity of the gratings. Figure 1 shows $\omega(x+y, x+y)\bar{\epsilon}$ spectra of both samples as well as that of an Al_{0.48}In_{0.52}As alloy sample. The spectrum of the bilayer exhibits a peak at 115 cm⁻¹ that is absent for the other two samples. Polarization measurements and phonon dispersion calculations based on a one dimensional elastic continuum (Rytov) model¹⁵ lead us to assign this peak to the first zone folded acoustic doublet (unresolved in the experiment). In the calculation, bulk values of the density and speed of sound were uncorrected for strain. In structures that exhibit alternating biaxial compression and tension, this may not be a bad approximation since the average sound velocity remains relatively unchanged. In GaSb/AlSb superlattices, discrepancies between experimental data and the Rytov model (uncorrected for strain) have been attributed to the nonlinearity of the bulk dispersion only.¹⁷ Values for the

density and sound velocity of InAs (AlAs) used in our calculation were 5.667 (3.7285) g/cm^3 and $3.834 (5.118) \times 10^5$ cm/s. These parameters give a value for the first zone folded mode that is approximately 10 cm^{-1} higher than the observed peak. Adjustment of the layer thicknesses by integral monolayers does not give better agreement with experiment. As discussed in reference 17, the nonlinearity of the bulk dispersion would account for observation of the folded mode at a lower energy than that predicted by a model which assumes a constant average sound velocity. All three scans show a peak near 190 cm^{-1} . For the alloy and bilayer samples this corresponds to a disorder activated LA mode and indicates some degree of imperfection in the case of the superlattice. On the other hand, a monolayer superlattice is expected to show a single folded mode at the energy of the bulk zone edge. In the monolayer scan this peak may thus be a zone folded acoustic mode rather than a disorder related feature. The optical region of the spectrum in all cases shows peaks arising from the vibrations of Al-As and In-As atomic pairs. The peak near 350 cm^{-1} in the alloy is due to the LO phonon of the InP substrate. The spectrum of the bilayer sample shows two peaks in the In-As vibration energy range, the one at 238 cm^{-1} arising from the $Al_{.48}In_{.52}As$ cap and the one at 249 cm^{-1} originating in the superlattice. In strained layer superlattices, quantum confinement and strain effects both contribute to the optical phonon energies. In unstrained materials like (GaAs)(AlAs) the phonon energy levels correspond to those of bulk at the discrete wavevectors given by $k_m = m\pi/(n+1)a$ where n is the number of

monolayers of width a , and $1 \leq m \leq n$. The model of Cerdeira, *et. al.*¹⁸ was used to estimate the strain shift of the LO phonons. Using the data in that reference for InAs, one arrives at frequency shift of approximately 13 cm^{-1} for the LO phonon for the lattice mismatch of 0.038, appropriate for InAs/ $\text{Al}_{.48}\text{In}_{.52}\text{As}$. Note that the frequency shift is positive. The expected shift due to quantum confinement is about 6 cm^{-1} , so that the observed shift of 8 cm^{-1} from the bulk InAs LO phonon energy is reasonable. For layers in tensile strain, the expected phonon energy shift is negative. If one assumes similar elastic properties of AlAs and GaAs, this value is expected to be about 15 cm^{-1} , which when added to the estimated quantum confinement shift of 12 cm^{-1} is close to the observed shift of 30 cm^{-1} . The optical phonon energies of the monolayer sample are virtually identical to those of the alloy.

To provide additional confirmation of structure and periodicity, x-ray diffraction measurements were made on both samples. The data were taken with a four circle diffractometer equipped with a rotating anode and copper target. Bent and flat graphite crystals were used as the incident and diffracted beam monochromators. The resulting increase in diffracted beam intensity facilitates observation of superlattice features in thin samples but requires sacrificing resolution. Figures 2 and 3 show the diffracted beam intensity as a function of reciprocal lattice index for the mono- and bilayer samples. In both cases the presence of $(h00)$ peaks (h odd), which are forbidden in the random alloy, confirms the additional (super)periodicity. In contrast to previous MBE

results for $(\text{InAs})_2(\text{AlAs})_2$, the bilayer sample studied here clearly exhibits a (900) diffraction peak.¹² For the two monolayer sample the satellite peaks correspond to a superperiod of 11.89 Å, close to the calculated value of 11.74 Å. Pairs of peaks near (200) and (600) are also evident and apparently arise from the unequal thickness of $(\text{InAs})_2$ and $(\text{AlAs})_2$. The splitting of the (100) and (300) peaks in the monolayer scan indicates a nonintegral monolayer thickness.⁷ From the positions of these peaks we deduce that n , the number of monolayers actually present, is equal to 1.17.⁷

Cross sectional high resolution and diffraction TEM images of the bilayer sample and diffraction images of the monolayer sample were obtained. Before examination, the samples were polished, dimpled and ion milled. The energy of the electron beam was 400 keV. Figure 4 is a high resolution cross sectional image of the two monolayer sample, clearly showing the compositional modulation. In this photograph, InAs (AlAs) layers appear dark (light). Although some interface nonuniformity is suggested, good overall homogeneity is indicated. Figures 5 and 6 show the diffraction patterns for the one and two monolayer samples, respectively. As in the x-ray data, superlattice satellites are evident.

In summary, we have grown high quality short period strained layer $(\text{InAs})_1(\text{AlAs})_1$ and $(\text{InAs})_2(\text{AlAs})_2$ superlattices by MEE. Their structural properties have been investigated using Raman scattering, x-ray diffraction and TEM. For the bilayer sample, acoustic phonons reveal the existence of the su-

perperiodicity and indicate some disorder, and the energies of the quantum confined optical phonons are consistent with the calculated strain. The spectrum of the monolayer sample showed no appreciable difference from the alloy. The x-ray data for the bilayer confirms the expected superperiod and reveals in the case of the monolayer the presence of some random alloy. TEM data give similar information.

The authors wish to thank J. Zhu for the TEM measurements and R. Jacowitz and Dr. S. Laderman of Hewlett-Packard Laboratories, Palo Alto, for the x-ray data. J. Berry is acknowledged for expert technical assistance. This work was supported, in part, by Innovative Science and Technology contract No. N00014-89-J-1311.

References

- [1] T. Yao: Japan. J. Appl. Phys. **22**, L680 (1983)
- [2] J. Singh, S. Dudley, B. Davies and K. K. Bajaj: J. Appl. Phys. **60**, 3167 (1986)
- [3] T. P. Pearsall, G. Beuchet, J. P. Hirtz, N. Visentin and M. Bonnet: in *GaAs and Related Compounds, Institute of Physics Conf. Ser. No. 56*, 639 (1980)
- [4] K. Seo, P. K. Bhattacharya and K. R. Gleason: Electron. Lett. **23**, 259 (1987)
- [5] C. Peng, M. I. Aksun, A. A. Kelterson, H. Morkoc and K. R. Gleason: IEEE Electron Device Lett. EDL-8, 24 (1987)
- [6] T. Itoh, A. S. Brown, L. H. Gammnitz, G. W. Wicks, J. D. Berry and L. F. Eastman: in *Proc. 12th Int. Symp. GaAs and Related Compounds*, 571 (1986)
- [7] T. Fukui and H. Saito: Japan. J. Appl. Phys. **23**, L521 (1984)
- [8] M. Razeghi, P. Maurel, F. Omnes and J. Nagle: Appl. Phys. Lett. **51**, 2218 (1987)
- [9] B. T. McDermott, N. A. El-Masry, M. A. Tischler and S. M. Bedair: Appl. Phys. Lett. **51**, 1830 (1987)
- [10] J. M. G érard, J. Y. Marzin, B. Jusserand, F. Glas, J. Primot: Appl. Phys. Lett. **54**, 30 (1989)
- [11] Y. Horikoshi, M. Kawashima and H. Yamaguchi: Japan. J. Appl. Phys. **27**, 169 (1987)
- [12] K. Nishi, T. Anan, Y. Ide, K. Onabe: J. Crystal Growth **95**, 202 (1989)
- [13] J. W. Matthews and A. E. Blakeslee: J. Crystal Growth, **27**, 118 (1974)
- [14] F. Houzay, C. Guille, J. M. Moison, P. Henoc, F. Barthe: J. Cryst. Growth **81**, 67 (1987)
- [15] C. Colvard, R. Merlin, M. V. Klein and A. C. Gossard: Phys. Rev. Lett. **43**, 298 (1980)
- [16] B. Jusserand, D. Paquet and A. Regreny: Phys. Rev. B **30**, 6245 (1984)
- [17] P. V. Santos, A. K. Sood, M. Cardona, K. Ploog: Phys. Rev. B **37**, 6381 (1988)

- [18] F. Cerdeira, C. J. Buchenauer, F. H. Pollak, M. Cardona: Phys. Rev. B 5, 580 (1972)

Figure Captions

Figure 1. Polarized Raman spectra of $(\text{InAs})_2(\text{AlAs})_2$, $(\text{InAs})_1(\text{AlAs})_1$ and $\text{Al}_{.48}\text{In}_{.52}\text{As}$ alloy.

Figure 2. X-ray diffraction scan of bilayer sample.

Figure 3. X-ray diffraction scan of monolayer.

Figure 4. High resolution cross sectional TEM image of bilayer.

Figure 5. TEM diffraction pattern of monolayer.

Figure 6 TEM diffraction pattern of bilayer.

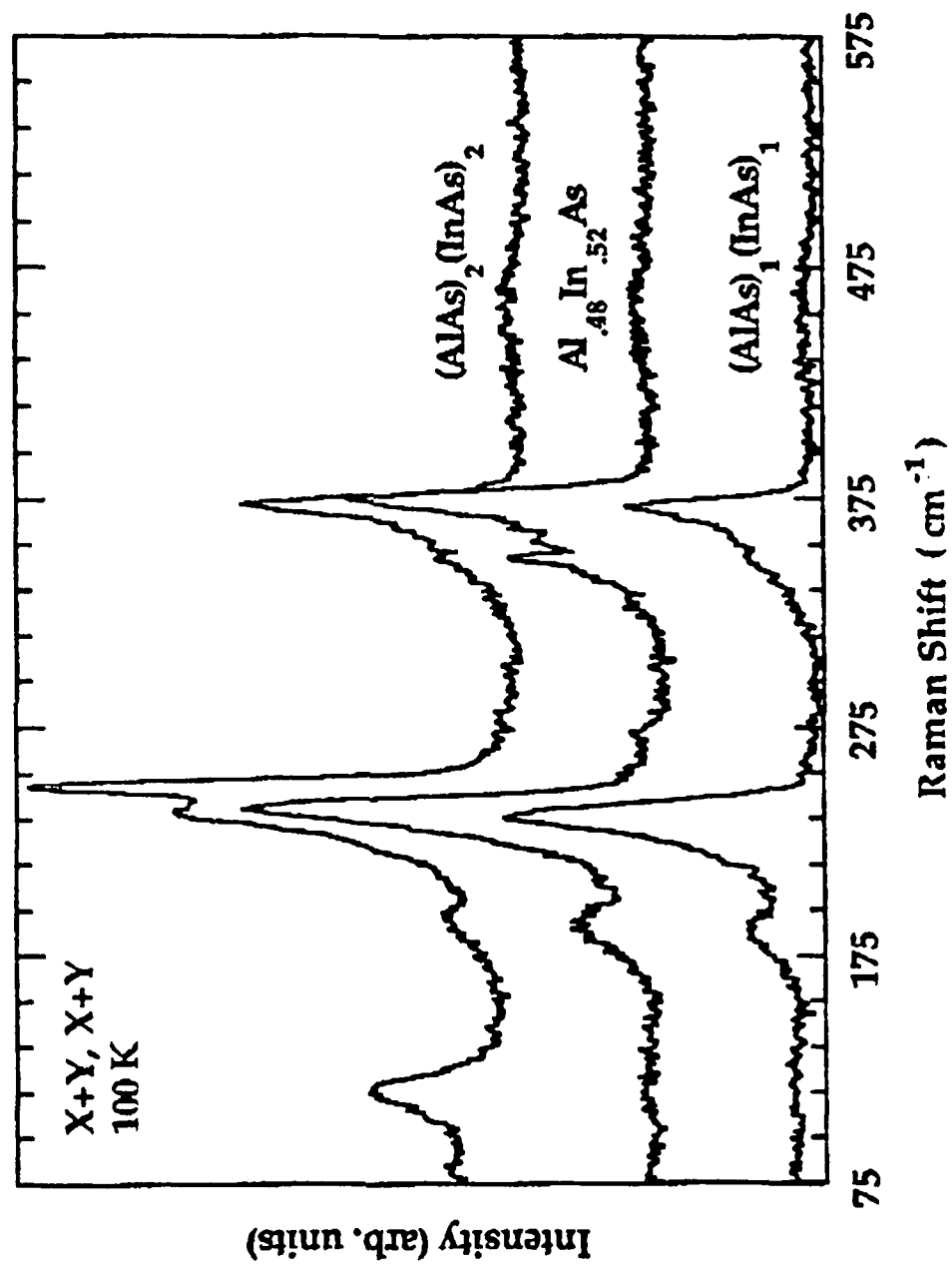
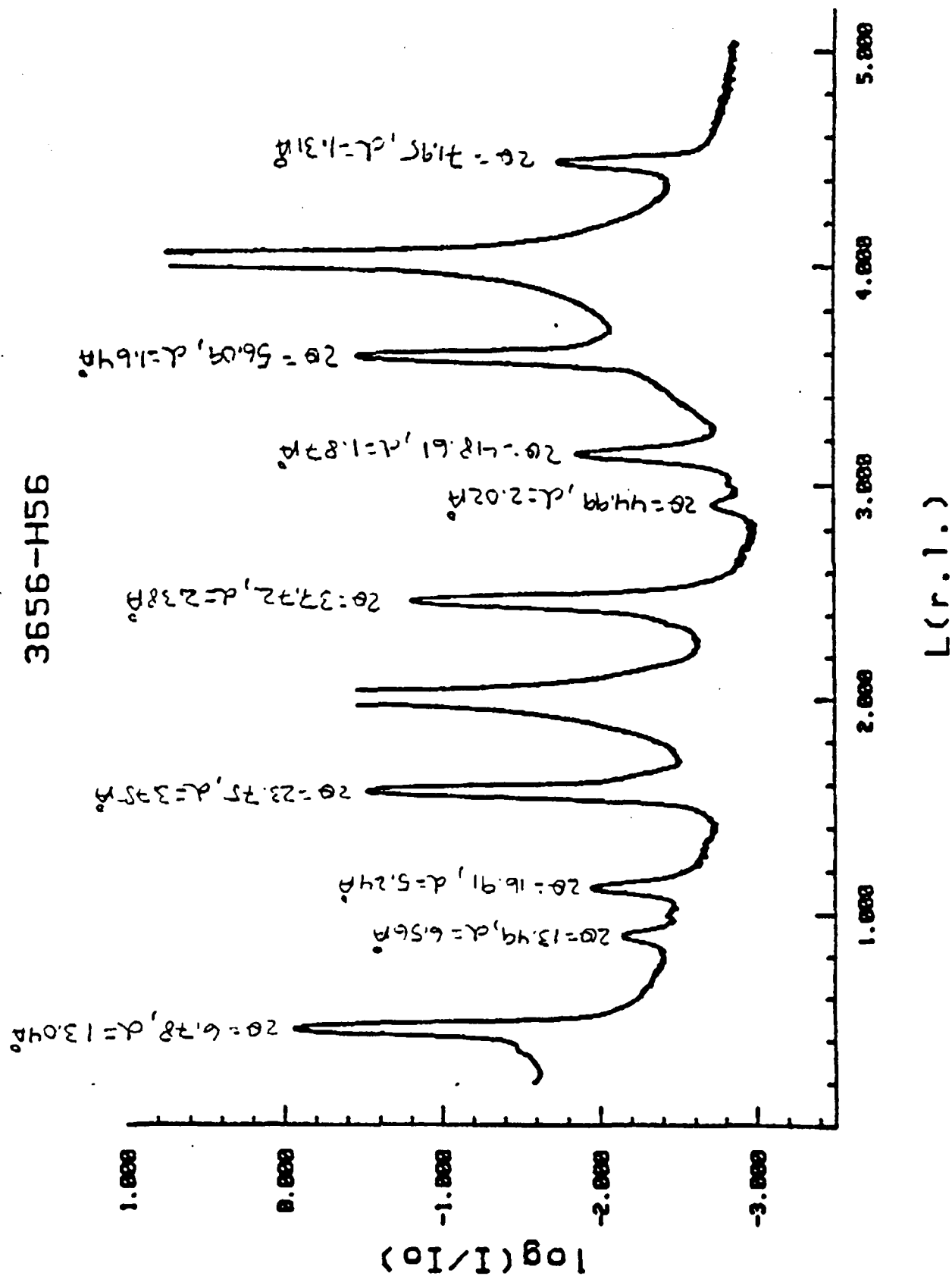


Fig. 1.5 2



~~Fig. 3~~

Fig. 3

3655-H55

